Rivista Italiana di Paleontologia e Stratigrafia
(*Research in Paleontology and Stratigraphy*)
vol. 123(1): 159-176. **March 2017**

CALCAREOUS NANNOPLANKTON RESPONSE TO THE LATEST CENOMANIAN OCEANIC ANOXIC EVENT 2 PERTURBATION

GIULIA FAUCHER[1*], ELISABETTA ERBA[1], CINZIA BOTTINI[1] & GABRIELE GAMBACORTA[1]

[1*]Corresponding author. Department of Earth Sciences, Università degli Studi di Milano, 20133 Milan, Italy. E-mail: giulia.faucher@unimi.it

To cite this article: Faucher G., Erba E., Bottini C. & Gambacorta G. (2017) - Calcareous nannoplankton response to the latest Cenomanian Oceanic Anoxic Event 2 perturbation. *Riv. It. Paleontol. Strat.*, 123(1): 159-176.

Key words: morphometry; coccoliths; Oceanic Anoxic Event 2; ocean acidification.

Abstract. Morphometric analyses were performed on *Biscutum constans*, *Zeugrhabdotus erectus*, *Discorhabdus rotatorius* and *Watznaueria barnesiae* specimens from five sections spanning the Cenomanian-Turonian boundary interval including Oceanic Anoxic Event (OAE) 2 (~ 94 Ma). The study provides evidence for size fluctuations and dwarfism of *B. constans* during OAE 2, followed by a partial recovery at the end of the event: this taxon appears to be the most sensitive species, with similar and coeval size trends in all the analyzed sections. Conversely, morphometry shows negligible or unsystematic coccolith variations in *Z. erectus*, *D. rotatorius* and *W. barnesiae*. The comparison of OAE 2 data with those available for the early Aptian OAE 1a and latest Albian OAE 1d, indicates that *B. constans* repeatedly underwent size reduction and temporary dwarfism, possibly implying that the same paleoenvironmental factors controlled calcification of *B. constans* during subsequent OAEs although the amplitude of *B. constans* coccolith reduction is significantly larger for OAE 1a than OAE 2.

Paleoceanographic reconstructions suggest that ocean chemistry related to the amount of CO_2 and toxic metal concentrations played a central role in *B. constans* coccolith secretion, while temperature and nutrient availability do not seem to have been crucial. Contrary to OAE 1a, *Z. erectus*, *D. rotatorius* and *W. barnesiae* appear to be substantially unrelated to OAE 2 paleoenvironmental stress, possibly because of different degrees of perturbation.

Introduction

The geological record of the Cretaceous world documents profound changes in the ocean-atmosphere system, including volcanic injection of large amounts of CO_2, super-greenhouse conditions, oceanic anoxia and eutrophication (e.g. Schlanger & Jenkyns 1976; Erba 2004; Hay 2009; Jenkyns 2010; Föllmi 2012; Bottini et al. 2015; Erba et al. 2015). Intervals of prolonged global anoxia, known as Oceanic Anoxic Events (OAE)s (Schlanger & Jenkyns 1976) were characterized by burial of unusually large amounts of organic matter during profound perturbations of the ocean-atmosphere system, similarly to current (and future) global changes.

The latest Cenomanian OAE 2 (~94 Ma) is arguably regarded as the most extreme paleoenvironmental stress related to the warmest climate of the past 150 My, characterized by an accelerated hydrological cycle, enhanced production and burial of organic matter, very high concentrations of volcanically-produced CO_2 and altered chemistry and structure of the oceans (see review provided by Jenkyns 2010). In the time interval encompassing OAE 2, calcareous nannoplankton were forced to face anomalous paleoceanographic and paleoclimatic conditions that induced extinctions and originations (e.g. Bralower 1988; Leckie et al. 2002; Erba 2004). Quantitative studies of nannofossil assemblages in various geological settings revealed differential abundance patterns of fertility-related species, in particular of *Biscutum constans* and *Zeugrabdothus erectus*. In general, an eutrophication episode was reconstructed at low latitudes (Hardas & Mutterlose 2007) while a shift to oligotrophic conditions was evidenced at mid-latitudes (Gale et al. 2000; Linnert et al. 2010, 2011). In the Western Interior Seaway (WIS) local changes controlled the trophic level across OAE 2 (Corbett & Watkins 2013).

In this work, we focus on size variations of four species, namely *Biscutum constans*, *Discorhabdus rotatorius, Watznaueria barnesiae* and *Zeugrabdothus erectus* in the Cenomanian-Turonian boundary interval (CTBI), and specifically across OAE 2. These taxa were previously studied through the early Aptian OAE 1a (Erba et al. 2010; Lübke et al. 2015; Lübke & Mutterlose 2016), the latest Albian OAE 1d (Bor-

Received: November 15, 2016; accepted: January 15, 2017

nemann & Mutterlose 2006) and the CTBI (Linnert & Mutterlose 2012) providing insights into coccolith size changes across OAEs. In particular, Erba et al. (2010) demonstrated that calcareous nannoplankton was extremely sensitive to ocean acidification associated to OAE 1a at low latitude sites in the Tethys and Pacific Oceans, allowing separation of most-, intermediate-, and least-tolerant taxa: dwarfism of *B. constans, Z. erectus* and *D. rotatorius* coccoliths was documented during OAE 1a but no significant changes in *W. barnesiae* dimension were detected, although more elliptical and malformed specimens were identified (Erba et al. 2010). Dwarfism of *B. constans* and *Z. erectus* was documented also across OAE 1a at higher latitudes (North Sea and Lower Saxony Basin, Lübke & Mutterlose 2016), but explained as the response to decreased light in surface waters under conditions of intense run off. In the same sections, *W. barnesiae* remained stable without significant size variations and interpreted as a robust species with respect to changes of sunlight penetration.

During OAE 1d, morphometry of *B. constans* specimens attested a decrease in mean length, while the average size of *W. barnesiae* coccoliths remained constant (Bornemann & Mutterlose 2006). Linnert & Mutterlose (2012) investigated nannofossil morphometry at two Deep Sea Drilling Project (DSDP) sites from Goban Spur in the Cenomanian-Turonian interval, although hiatuses across OAE 2 hampered the reconstruction of detailed size variations in the CTBI. However, slightly smaller *Biscutum* specimens were observed in the lower Turonian compared to the upper Cenomanian interval, while no significant changes in size were detected for genus *Watznaueria*.

Sections from various oceanic basins were selected on the basis of their stratigraphic characterization, ensuring relatively high resolution and correlation at supra-regional scale. The main objectives of this study are: i) the assessment of size variations of *B. constans*, *D. rotatorius, W. barnesiae* and *Z. erectus* across OAE 2; ii) the evaluation of timing and type of reactions of phytoplankton calcification through progressively stressing conditions and their demise; iii) the identification of global, regional and local response to paleoenvironmental perturbations; iv) the evaluation of synchroneity or diachroneity of nannoplankton variations versus paleoenvironmental changes; v) implementation of paleoecological reconstructions of abiotic and biotic parameters influencing coccolith secretion across OAEs. In particular, we want to test the following hypotheses: (1) did short-term fluctuations in coccolith morphometry follow transient changes in climate and ocean chemistry across OAE 2?; (2) did *B. constans*, *D. rotatorius, W. barnesiae* and *Z. erectus* respond to OAE 2 perturbations similarly to other OAEs?; (3) were single or concomitant paleoenvironmental factors influencing calcareous nannoplankton calcification?; (4) were changes in coccolith size abrupt or gradual, especially at the onset and demise of OAE 2?; (5) were the paleolatitudes discriminating for coccolith size ?

Location/studied sections

We studied five stratigraphic sections covering the CTBI (Figs 1 and 2), including Eastbourne (East Sussex, England), Clot Chevalier (Vocontian Basin, France), Novara Di Sicilia (northeastern Sicily, Italy), Rock Canyon (Pueblo, Colorado, USA) and Cuba (northern-central Kansas, USA) sections from the WIS. These sections were chosen based on availability of integrated stratigraphy granting a good time control derived from C-isotopic stratigraphy and biostratigraphy.

Eastbourne is the thickest section covering the CTBI in the Anglo-Paris Basin (Gale 1995, 1996; Gale et al. 1999; Paul et al. 1999). The studied outcrop was sampled at Gun Gardens and consists of a 27 m-thick section comprising three lithological units: Grey Chalk (rhythmically bedded marly chalk), Plenus Marls (greenish grey marls and clay-rich chalk) and White Chalk (coccolith and calcisphere-dominated nodular limestone). Samples analyzed were collected during the CT-Net Project and nannofossil biostratigraphy combined with chemostratigraphy was published in Tsikos et al. (2004): OAE 2 is constrained by the last occurrences of *Corollithion kennedyi* and *Axopodorhabdus albianus* and the first occurrence of *Quadrum gartneri* at OAE 2 onset and end, respectively. These nannofossil events are consistent with more recent biostratigraphic data by Linnert et al. (2011).

The Novara di Sicilia section consists of a 19 m-thick stratigraphic interval measured through an olistolith within a melange of the Argille Varicolori (Scopelliti et al. 2008). From a lithological

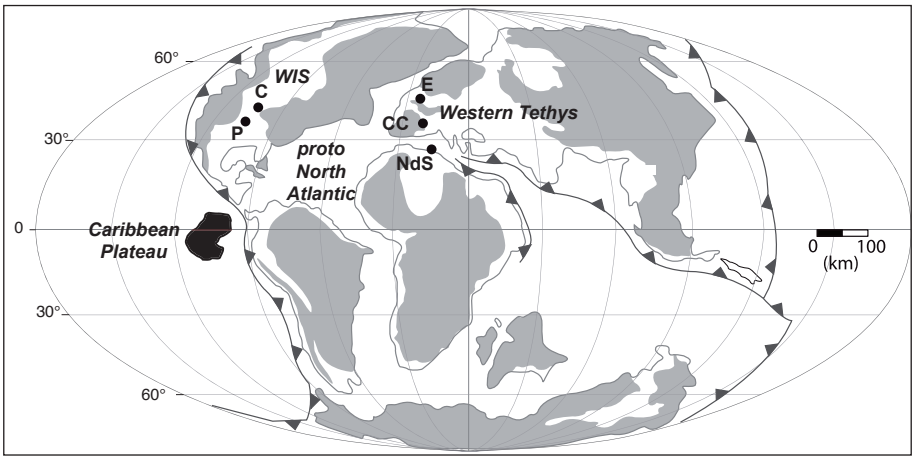

Fig. 1 - Paleo-location of the studied sections at ~ 94 Ma (late Cenomanian). E = Eastbourne, CC = Clot Chevalier, NdS = Novara di Sicilia, P = Pueblo and C = Cuba, WIS = Western Interior Seaway. The paleo-map is from Du Vivier et al. (2014).

point of view, the succession can be divided into three parts: a lower part with alternations of thick marly limestone with light and dark marlstone, an intermediate portion with thinner light-colored strata and an upper part of black shale alternating with dark marlstone and claystone. The nannofossil and planktonic foraminiferal biostratigraphy, integrated with C-isotopic stratigraphy (Scopelliti et al. 2008) indicate that the Novara di Sicilia section contains only the lower part of the Bonarelli Level equivalent and the underlying interval. Specifically, the outcrop ends shortly above $\delta^{13}C_{org}$ peak B indicating that only the onset and early part of OAE 2 are represented.

The Clot Chevalier section is located in the Vocontian Basin (southeastern France) that was a part of the hemipelagic intrashelf basin of the European Tethyan passive margin (Wilpshaar et al. 1997). The 35 m analyzed section consists of an alternation of dark grey marlstone and light grey limestones (Falzoni et al. 2016). The local equivalent of the "Bonarelli Level" in the Clot Chevalier section is represented by the "Thomel Level", which is characterized by laminated organic-rich sediments (from 3 to 31 meters from the base of the section) (Falzoni et al. 2016). At the base of Th1 unit, the presence of a borrowed sharp surface reveals the existence of a hiatus in the lower part of the section. Furthermore, within units Th1 and Th2, a condensed stratigraphic level has been observed and interpreted as an interval of very low sedimentation rate or sedimentation interruption. Nannofossil biostratigraphy was achieved by Russo (2014).

The Rock Canyon-Pueblo and the Cuba sections are both from the WIS where the Cenomanian/Turonian boundary lies within the Bridge Creek Limestones Member of the Greenhorn Formation. The Rock Canyon section is located in southern-central Colorado near Pueblo, along the Arkansas River; it was ratified as the global boundary stratotype section and point (GSSP) for the base of the Turonian Stage (Kennedy et al. 2005). Here, the Bridge Creek Limestones consist of alternating pelagic chalk and limestone and C_{org}-rich beds (marlstone and calcareous shale), mainly bioturbated, with laminated and sublamintated units. The Rock Canyon section has been intensively investigated for litho-, bio-, chemo- stratigraphy and for paleoecological and paleoenvironmental reconstructions (Leckie 1985; Pratt 1985; Pratt et al. 1993; Bralower 1988; Kennedy 2000; Keller & Pardo 2004; Snow et al. 2005; Sageman et al. 2006; Corbett & Watkins 2013). The analyzed interval goes from 0.3 m to 10.2 m: samples from the pre-OAE 2 interval were not available.

The Cuba section in northern-central Kansas, is about 600 km East of the Rock Canyon section. Equivalent strata around Cuba consist of more fine-grained calcareous to chalky shale within the Jetmore Chalk and Pfeifer Shale Members of the Greenhorn Formation. These two members are dominated by marlstone and calcareous shale (Bowman & Bralower 2005). At the Cuba section the stratigraphic control is based on integrated litho-, chemo-, bio- stratigraphy (Hattin 1975, 1985; Bowman & Bralower 2005; Eleson & Bralower 2005; Desmares et al. 2007; Corbett & Watkins 2013; Corbett et al. 2014). The analyzed samples were previously investigated for chemo- and biostratigraphy by Bowman & Bralower (2005) and Eleson & Bralower (2005).

Methods

Calcareous nannofossils were investigated in smear slides under light polarizing microscope, at 1250X magnification. Smear slides were prepared using standard techniques (Bown & Young 1998) without centrifuging and/or ultrasonic cleaning in order to retain the original sediment composition. A small fraction of sediment was powdered in an agate mortar with bidistillate water; a few drops of the suspension were extracted with a pipette and spread over a slide, leaving to dry on a hot plate. The dried suspension was sealed on a glass slide with Norland Optical adhesive.

The nannofossil preservation was carefully assessed in order to avoid diagenetically altered material. In fact, partial dissolution and/or overgrowth have the potential to artificially decrease or enlarge the coccolith size, respectively. This is particularly relevant for the delicate *Biscutum, Zeugrhabdotus* and *Discorhabdus* coccoliths that are diagenetic-prone (e.g. Thierstein 1980). Accurate screening of preservation was achieved under light polarizing microscope to ascertain the degree of etching and/or overgrowth. Moreover, individual *B. constans, Z. erectus, D. rotatorius* and *W. barnesiae* coccoliths considered for morphometry were selected based on their complete and continuous outline and lack of crimping due to etching or overgrowth. We also tested the potential control - and its degree - of lithology on coccolith preservation, because marlstones normally contain the best preserved nannofossil assemblages, while coccoliths are often affected by overgrowth in limestones and by etching in carbonate-poor lithotypes (Thierstein & Roth 1991).

Morphometric analyses were performed on a total of 53 samples from Eastbourne, 37 from Clot Chevalier, 40 from Novara di Sicilia, 21 from Pueblo and 18 from Cuba sections. For each sample 30 specimens of *B. constans, Z. erectus* and *D. rotatorius* and 50 specimens of *W. barnesiae* were digitally photographed in random fields of view. Samples containing less than 30 specimens of selected species were not included in the analyses. Morphometry of *W. barnesiae* was conducted with a lower sampling resolution.

Images of coccolith specimens were taken using a camera mounted on a Leitz Laborlux light microscope. Length and width (the diameter for *D. rotatorius*) of coccolith distal shield were measured on digital images using ImageJ64 software. A total of 4740 of *B. constans*, 4500 of *Z. erectus,* 4770 of *D. rotatorius* and 7500 of *W. barnesiae* were measured. The error of measurements is of $\pm$ 0.08 μm.

Data were statistically elaborated, using R software, to obtain mean, median, maximum and minimum values, 25% and 75% percentile, 95% confidence intervals, standard deviations, Pearson correlation coefficient (r) and the linear regression function. Moreover, the analyses of variance (ANOVA) and Tukey post hoc tests were performed with R software in order to determine if size variations are statistically significant.

Results

In all studied samples preservation is moderate and only very minor indications of etching and overgrowth were sporadically detected. Our diagenetic estimates are in agreement with evaluation of dissolution and overgrowth previously published for nannofossil assemblages. In particular, at Pueblo, Bralower (1988) and Corbett et al. (2014) documented moderate preservation as assessed in this study. Similarly, Linnert et al. (2011) and Scopelliti et al. (2008) observed moderately preserved assemblages at Eastbourne and Novara di Sicilia, respectively. Good to excellent preservation was documented for nannofloras of the Cuba section (Eleson & Bralower 2005).

Samples analyzed from the five sections randomly consist of various lithologies, all yielding very similar degree of preservation and there is no correlation between coccolith size and carbonate content. Diagenetic modifications were certainly different for the studied sections were deposited at different paleo-water depths and in various geological settings, under diverse sedimentation regimes. However, similar patterns in nannofossil assemblages with coexistence of delicate and robust species points to negligible diagenetic influence. Moreover, we underline that morphometric data were gathered only for complete specimens without signs of corrosion or overgrowth in the outline.

The adopted stratigraphic framework is based on the $\delta^{13}C$ curve integrated with nannofossil biostratigraphy (Fig. 2). Specifically, peaks A, B and C of $\delta^{13}C$ curve (Pratt et al. 1985; Tsikos et al. 2004; Jarvis et al. 2006; Gambacorta et al. 2015) are taken as key-levels for dating and correlations. As discussed by Jarvis et al. (2006, 2011), peak A represents the acme of the first shift towards $\delta^{13}C$ positive values. It is followed by a trough and a subsequent increase culminating at $\delta^{13}C$ peak B marking the onset of the so-called plateau. The end of the OAE 2 C-isotopic anomaly correlates with $\delta^{13}C$ peak C followed by the decrease back toward pre-excursion $\delta^{13}C$ values (Tsikos et al. 2004). In the next sub-chapters, the size fluctuations of *B. constans, Z. erectus, D. rotatorius* and *W. barnesiae* coccoliths are presented for every section (Fig. 3, Supplementary Tab. 1). Since the correlation of length and width of *B. constans, Z. erectus* and *W. barnesiae* coccoliths evidences a high Pearson correlation coefficient (Supplementary Fig. S1, S2, S3), only the length is plotted and used for tracing size changes.

Eastbourne

Coccoliths of *B. constans, Z. erectus* and *D. rotatorius* show similar size trends through the Eastbourne section (Fig. 3a). Specifically, at the OAE 2 onset, *B. constans, Z. erectus* and *D. rotatorius* evidence a decrease in size becoming smaller than the mean values (blue line). Subsequently, a slight increase

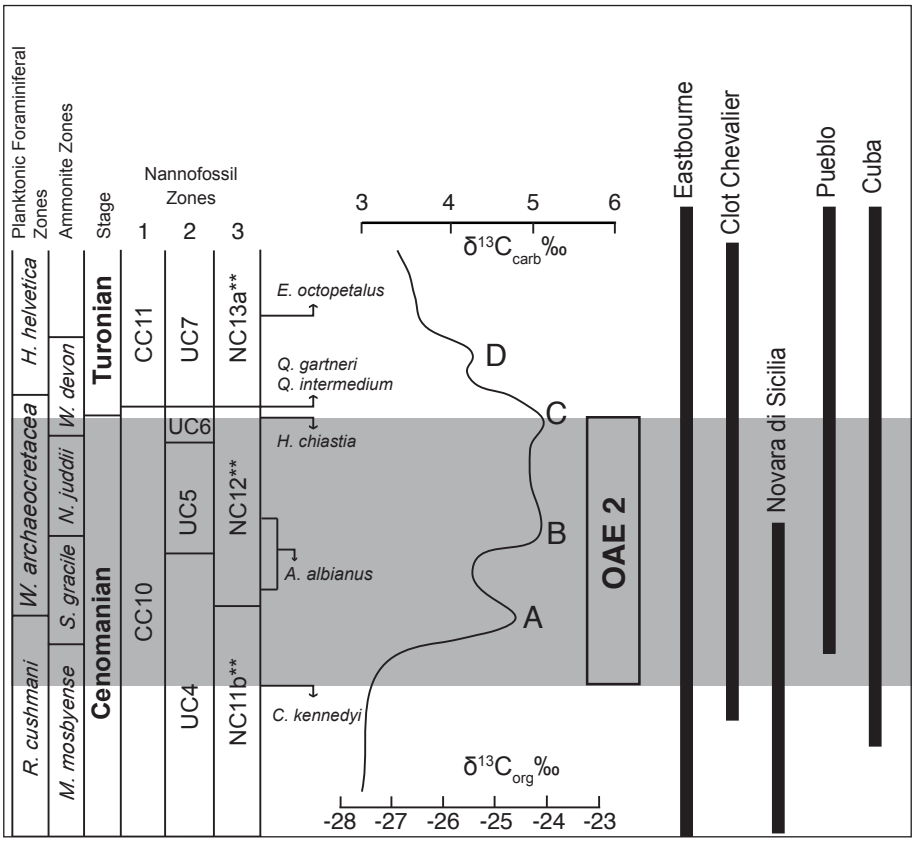

Fig. 2 - Stratigraphic ranges of the studied sections through the late Cenomanian-early Turonian time interval. Nannofossil zonations discussed in Gambacorta et al. (2015). 1 = Sissingh (1977); 2 = Burnett (1998), 3 = Gambacorta et al. (2015).

in coccolith size is detected and higher values are reached across $\delta^{13}C$ peak A. Successively, coccoliths display a reduction in size reaching minimum values around $\delta^{13}C$ peak B. In the uppermost part of the section, coccoliths evidence an increase in size becoming slightly larger than the mean size. *W. barnesiae* is rather constant through the event (see Supplementary Tab. 1), although a minor increase in size is observed in the interval between $\delta^{13}C$ peaks C and D (Fig. 3a).

Clot Chevalier

In the Clot Chevalier section, the interval preceding OAE 2 is rather thin and only a few samples were available for the analyses. Size trends are well expressed in *B. constans* and *D. rotatorius* (Fig. 3b). From the base, *B. constans* and *D. rotatorius* show a relative increase in size compared to the mean length-diameter. *B. constans* and *D. rotatorius* maintain bigger sizes in the lowermost part of OAE 2 and then sizes progressively decrease just after $\delta^{13}C$ peak A, reaching relative minimum values around $\delta^{13}C$ peak B. *B. constans* displays values close to average in the upper part of $\delta^{13}C$ plateau up to peak C where, along with *D. rotatorius,* there's a minor increase in size. Size fluctuations are less evident in *Z. erectus* and *W. barnesiae* that do not show significant trends through the event. However, *Z. erectus* shows a minor increase in size just after $\delta^{13}C$ peak C.

Novara di Sicilia

In the Novara di Sicilia section, only the pre-OAE 2 interval and the first part of the event are represented (Fig. 3c). In the pre-OAE 2 interval size values of *B. constans, Z. erectus* and *D. rotatorius* are erratic (Fig. 3c) with successive increases and decreases in size trends. In the first part of OAE 2, after a basal interval barren of calcareous nannofossils, *B. constans* shows coccoliths larger than the mean size and subsequently a trend towards smaller coccoliths, followed by a recovery in size around $\delta^{13}C$ peak A. A final size decrease ends with a relative minimum around $\delta^{13}C$ peak B.

Z. erectus and *D. rotatorius* coccoliths display erratic values through OAE 2 and *W. barnesiae* specimens show values around average through the studied interval.

Cuba

In the lowermost portion of this section, only a few samples were available to characterize the pre-OAE 2 interval (Fig. 3d). Maximum coccolith

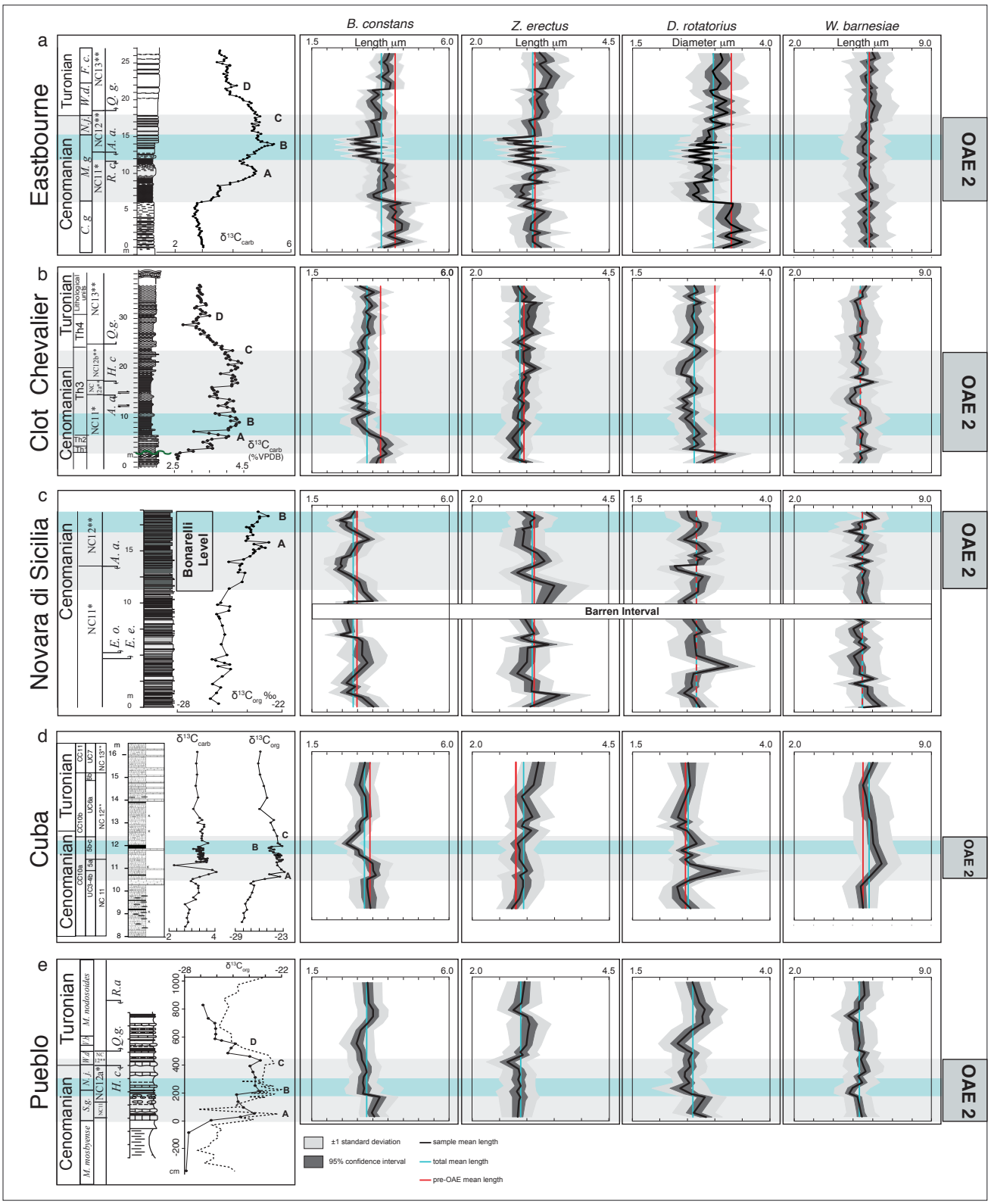

Fig. 3 - Variations of *B. constans*, *Z. erectus* and *W. barnesiae* length, and *D. rotatorius* diameter against $\delta^{13}C$ curve during OAE 2 at Eastbourne, Clot Chevalier, Novara di Sicilia, Pueblo Rock Canyon and Cuba. $\delta^{13}C$ and nannofossil zones at Eastbourne after Tsikos et al. (2004); Clot Chevalier $\delta^{13}C$ curve after Falzoni et al. (2016), nannofossil zones after Russo (2014); $\delta^{13}C$ and nannofossil zones at Novara di Sicilia after Scopelliti et al. (2008); $\delta^{13}C$ at Pueblo Rock Canyon after Snow et al. (2005), nannofossil zones after Russo (2014); Cuba $\delta^{13}C$ after Bowman and Bralower (2005), nannofossil zones after Eleson and Bralower (2005) integrated following Gambacorta et al. (2015).

values of *B. constans* are observed around $\delta^{13}C$ peak A followed by a decrease in size reaching minimum values around $\delta^{13}C$ peak B. In the upper part of the section, above $\delta^{13}C$ peak C, an increase in coccoliths is observed with values similar to the mean.

Coccoliths of *D. rotatorius* display a well-defined size peak at the onset of OAE 2 around $\delta^{13}C$ peak A, whereas *Z. erectus* dimensions are very similar to the mean size values with a gradual increase towards larger coccoliths recorded after $\delta^{13}C$ peak C. *W. barnesiae* doesn't show significant size changes, although an increase was observed in the lower part of OAE 2.

Pueblo

In the lowermost part of OAE 2 at Pueblo, an increase in size is observed in *B. constans* and *D. rotatorius* showing larger coccoliths around $\delta^{13}C$ peak A (Fig. 3e). Both *B. constans* and *D. rotatorius* display a decrease in size, reaching minimum values around $\delta^{13}C$ peak B and remaining small through the upper part of OAE 2 and overlying interval. A return to larger coccoliths was recorded after $\delta^{13}C$ peak D. *Z. erectus* and *W. barnesiae* show minor changes in size; however, smaller coccoliths of *Z. erectus* were observed at the end of the isotopic plateau and a slight decrease in size of *W. barnesiae* specimens correlates with $\delta^{13}C$ peak B.

Coccolith morphometry

Among analyzed species, *B. constans* shows distinct and coeval size fluctuations through OAE 2 in all studied sections, while *D. rotatorius*, *Z. erectus* and *W. barnesiae,* record only minor and isolated size variations at different stratigraphic levels. Mean length of *B. constans* (Supplementary Tab. 1) varies depending on latitude: coccoliths are bigger at highest latitude (i.e. Eastbourne) and progressively decrease southwards, reaching minimum values at lowest latitude sections (i.e. Novara di Sicilia). Within the studied sections, the main size features of *B. constans* can be summarized as follow:

larger coccoliths characterize the pre-OAE 2 interval;

a minor decrease in size correlates with the onset of OAE 2;

an increase in size trend reaches a maximum around $\delta^{13}C$ peak A;

a decrease in size trends culminates with dwarf coccoliths at $\delta^{13}C$ peak B;

a relative recovery in size marks the post – OAE 2 interval, although without reaching pre-event sizes.

The ANOVA and Tukey post hoc test were applied to coccolith morphometric data in order to evaluate if *B. constans* means are significantly different in the ten intervals identified within the $\delta^{13}C$ curve (Supplementary Tab. 2, Fig. S4): 1) pre-positive excursion; 2) initial rise; 3) peak A; 4) trough between peak A and peak B; 5) peak B; 6) plateau; 7) peak C; 8) decreasing values after peak C; 9) peak D; 10) further decrease after peak D. Statistical analyses evidence that, in every section, *B. constans* is always significantly smaller ($p < 0.05$, Supplementary Tab. 2) in interval number 5 corresponding to $\delta^{13}C$ peak B compared to interval number 1 (pre-OAE 2) and interval number 3 ($\delta^{13}C$ peak A).

Discussion

Calcareous nannoplankton calcification and OAE 2 perturbation

Morphometric and statistical analyses indicate consistent and significant changes in coccolith size of *B. constans* in all studied sections. We exclude a diagenetic control since the investigated successions yield rather homogenous moderate preservation, belong to different settings and underwent diverse diagenetic paths. Measured coccoliths are complete with no evidence of corrosion or overgrowth in the outline and the co-occurrence of incoherent size variations in different taxa is further evidence for disregarding diagenetic modifications.

Our morphometric data highlight latitude-related changes in *B. constans* size, being its coccoliths bigger at highest latitude (Eastbourne section) and progressively smaller southwards, with minimum values at lowest latitude (Novara di Sicilia section). Such findings are consistent with patterns observed in Cenozoic (Herrmann & Thierstein 2012) and Holocene (Herrmann et al. 2012) assemblages indicating changes in coccolith size across latitudes.

In order to understand the role of complex environmental stress of OAE 2 on *B. constans* size variations, we first take under consideration the multiproxy data available for the WIS and Eastbourne sections (Fig. 4). The record of pCO_2 concentrations derived from stomata in fossil leaves

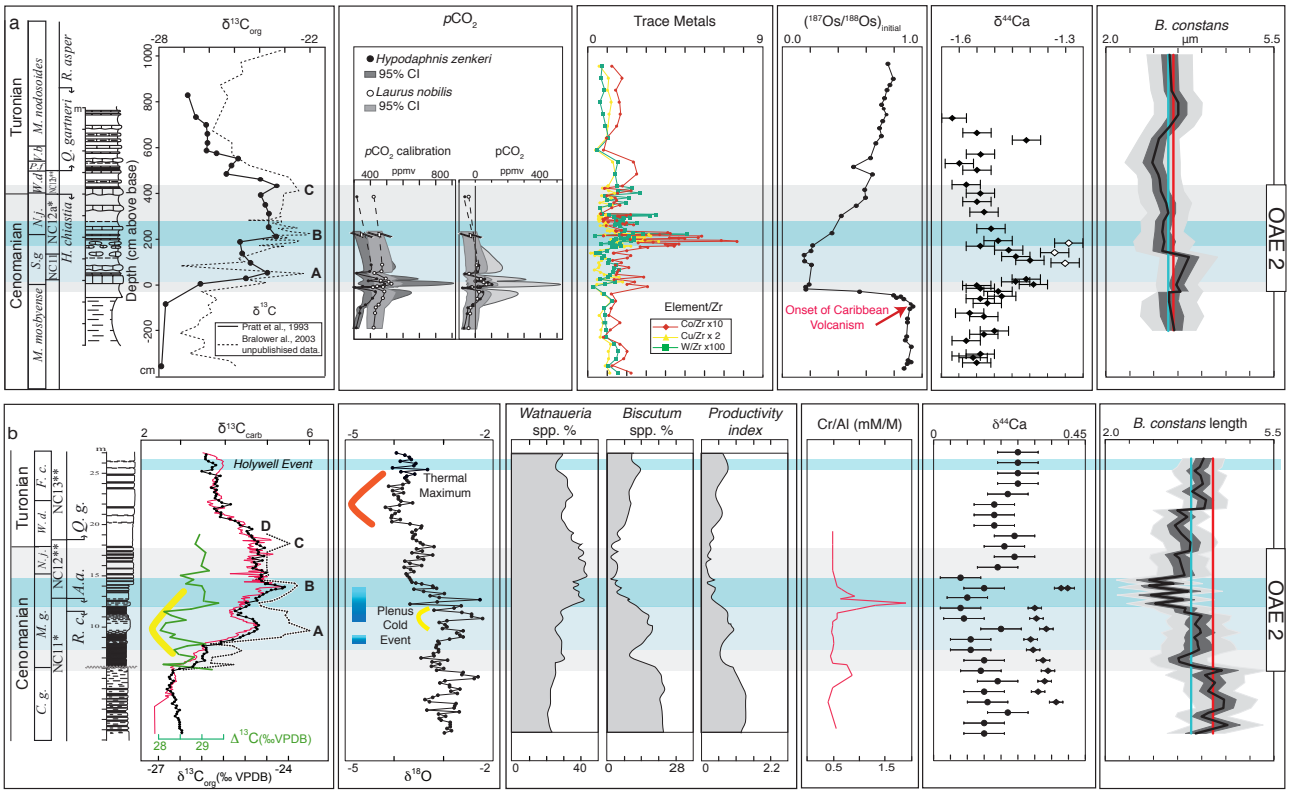

Fig. 4 - Synthesis of major geological events in the late Cenomanian – early Turonian interval a) WIS $\delta^{13}C$ curve (Snow et al. 2005); pCO_2 reconstruction (Barclay et al. 2010); trace metals (Snow et al. 2005); osmium-isotope signature (Du Vivier et al. 2014); calcium-isotope signature (Du Vivier et al. 2015); composite *B. constans* morphometric curve (this study): pre-OAE 2 interval data from Cuba section, OAE 2 and post OAE 2 interval from Pueblo Rock Canyon; b) Eastbourne section $\delta^{13}C$ curve (Tsikos et al. 2004) and $\delta^{13}C$ curve (Jarvis et al. 2011); $\delta^{18}O$ (Tsikos et al. 2004), cooler pulses during Plenus Cold Event (Jenkyns et al. 2016); relative abundance of *Watznaueria, Biscutum* and productivity index (Linnert et al. 2011); Cr/Al (Pearce et al. 2009); calcium-isotope signature (circle = $\delta^{44/42}Ca$, Blättler et al. 2013; diamonds = $\delta^{44/42}Ca$ Du Viver et al. 2015); *B. constans* morphometric curve (this study).

of the WIS area is limited to the first part of the C-isotopic anomaly (Barclay et al. 2010) associated with a long-term increase in pCO_2 interrupted by two relative lows. It was hypothesized that volcanic activity started to influence atmospheric CO_2 levels before the OAE 2 onset (Fig. 4a; Barclay et al. 2010): an increase by 20%, equivalent to a rise of 60-300 ppm, was attributed to a massive magmatic episode occurring some 500 kyrs in advance of the positive C-isotopic excursion that defines OAE 2 (Barclay et al. 2010). A distinct low in atmospheric CO_2 of about 25-26% (Barclay et al. 2010; Sinninghe Damstè et al. 2008) was documented at the stratigraphic level of $\delta^{13}C$ peak A, followed by a further increase up to the middle part of OAE 2 (Barclay et al. 2010).

Osmium isotopic signature moves towards less radiogenic values approximately 30-40 kyrs before OAE 2 onset and was attributed to an input of unradiogenic Os from a mantle source, thus suggestive of an intense submarine volcanism continuing through the first phase of OAE 2 (Du Vivier et al. 2014).

In the Pueblo section, Snow et al. (2005) documented a first relative increase and then a peak in trace metals at the onset of OAE 2 and at $\delta^{13}C$ peak B, respectively (Fig. 4a). The presence of these metal abundance anomalies needs an explanation other than influx of terrigenous input and the most reliable hypothesis is the release of magmatic fluids in event plumes (Snow et al. 2005). The metal-rich intervals are more abundant in the less volatile and more reactive elements (such as Sc, Co, Mn and Fe) and this is in good agreement with the position of the Caribbean Plateau, which was proximal to the WIS area. Cuba and Pueblo sections are, as expected, rich in a wide range of near-field and far-field elements. In the Eastbourne section, a relative increase in chromium (Cr/Al) was documented at the onset of OAE 2 (Fig. 4b) and a maximum precedes $\delta^{13}C$ peak B (Pearce et al. 2009). Shape and stratigraphic levels of both Cr enrichments at Eastbourne and Pueblo point to the Caribbean hydrothermal events (Pearce et al. 2009) associated with OAE 2.

At Eastbourne, temperature fluctuations were reconstructed using the O-isotopic record (Pearce et al. 2009; Jarvis et al. 2011): a relative warming correlates with the onset of OAE 2 and is interrupted by the Plenus Cold Event (Fig. 4b) associated with a temporary spread southwards of North boreal biota (including the index belemnite *Praectinocamax plenus*) (Pearce et al. 2009; Jarvis et al. 2011; Jenkyns et al. 2016). The middle-late part of OAE 2 is then characterized by increased paleotemperature culminating with the "early Turonian thermal maximum" just after $\delta^{13}C$ peak D (Jarvis et al. 2011). A shift towards lower $\delta^{44}Ca$ and $\delta^{7}Li$ values indicates accelerated weathering at the beginning of the OAE 2 C-isotopic anomaly (Blättler et al. 2011; Pogge von Stradmann et al. 2013), reaching a maximum around $\delta^{13}C$ peak B, some 200-300 kyrs after the volcanism onset (Pogge von Stradmann et al. 2013).

At Eastbourne and in the WIS areas, Du Vivier et al. (2015) documented a transient increase of $\delta^{44}Ca$ at the beginning of $\delta^{13}C$ anomaly: CO_2-induced ocean acidification during the Caribbean LIP eruption was proposed as the potential cause of such $\delta^{44}Ca$ positive shifts (Du Vivier et al. 2015).

Previous studies of nannofossil assemblages of the Eastbourne (Linnert et al. 2011) (Fig. 4b) and WIS (Corbett & Watkins 2013) sections showed partially contrasting data. Yet, a general picture of suppressed abundances of the fertility-taxa *B. constans* and *Z. erectus* was derived for mid-latitude shelf and epeiric settings through OAE 2 (Corbett & Watkins 2013). However, in the Cuba section, an increase of the higher-fertility nannofossil species was detected, suggesting local meso- to eutrophic conditions in the eastern margin of the WIS (Corbett & Watkins 2013). Paleoenvironmental perturbations in the CTBI reconstructed at Eastbourne and in the WIS are consistent with results gathered in other sections and used for global characterization of OAE 2 (Jenkyns 2010) in terms of paleoCO_2 fluctuations, climate moving to global warming, enhanced primary productivity due to increased nutrient fluxes and upwelling as well as ocean acidification.

Our nannofossil morphometric data may provide insights into the comprehension of type and rate of reactions of phytoplankton calcification through progressively stressing conditions and their demise.

We notice that short-term fluctuations in morphometry follow transient changes in climate and ocean chemistry. In particular, the reconstructed early increase in pCO_2 shortly prior to and at the beginning of OAE 2, associated with initial volcanism, correlates with the first decrease in size of *B. constans* coccoliths (Fig. 4 and Supplementary Fig. S4). A short-lived return to relatively larger coccoliths falls around $\delta^{13}C$ peak A, in the interval of the Plenus Cold Event and reconstructed lower pCO_2.

The subsequent decrease in *B. constans* size culminating in dwarfism across $\delta^{13}C$ peak B (Fig. 4 and Supplementary Fig. S4) correlates with metal enrichments and a significant temperature rise. Only a partial return to pre-OAE 2 sizes was observed in *B. constans* coccoliths after $\delta^{13}C$ peak D, suggesting the persistence of stressing conditions in the earliest Turonian characterized by high paleotemperatures known as the "early Turonian thermal maximum" (Jarvis et al. 2011).

As for living coccolithophores (Riebesell et al. 2000; Beaufort et al. 2011; Müller et al. 2011, 2012; Hoffmann et al. 2012; Sett et al. 2014), the main paleoenvironmental factors influencing calcareous nannoplankton calcification in the Cretaceous were presumably nutrient availability, sea surface temperature, carbonate chemistry, ocean acidification, toxic trace metals, competition with other organism and salinity (Erba 2004, 2006; Mutterlose et al. 2015). Linnert & Mutterlose (2012) highlighted a decrease in size of *Biscutum* specimens during OAE 2 at oceanic sites from northeastern Atlantic Ocean. The associated decrease in abundance of *Biscutum* suggested that the reduction in size occurred under oligotrophic conditions (Linnert & Mutterlose 2012). We found a similar relationship at Eastbourne and Pueblo (Figs 3, 5), but in the Cuba (Corbett & Watkins 2013) and Novara di Sicilia (Scopelliti et al. 2008) sections, the analogous decrease in *B. constans* coccolith size and dwarfism around $\delta^{13}C$ peak B, occurred under high nutrient availability (Scopelliti et al. 2008; Corbett & Watkins 2013). Therefore, the trophic level of surface water cannot be ascribed as the trigger of reduced calcification.

A cool-water preference was implied for *B. constans* (Lees et al. 2005) and may explain the increase in size of *B. constans* coccoliths around $\delta^{13}C$ peak A, during the Plenus Cold Event (Jenkyns et al. 2016) that is a global scale SST decrease of about 4°C (Voigt et al. 2004; Pearce et al. 2009). Conversely, the abundance and size decrease recorded

in *B. constans* coccoliths at $\delta^{13}C$ peak B are associated to a SST increase of ~ 6°C (Voigt et al. 2004; Pearce et al. 2009). However, it is dubious that *B. constans* calcification was directly controlled by SSTs, since the full recovery in size started just after $\delta^{13}C$ peak D under hot conditions of the "early Turonian thermal maximum". Indeed, the preference of *B. constans* for cooler surface-waters was previously questioned (e.g., Linnert & Mutterlose 2012) and, indeed, we notice that *B. constans* was very abundant during OAE 2 in the tropical Atlantic (Hardas & Mutterlose 2007) characterized by SSTs up to 35°C and in the earliest Turonian under the highest SSTs (Forster et al. 2007) recorded in the Boreal area (Linnert et al. 2010, 2011).

It is feasible that some acidification of seawaters postulated for the early phase of OAE 2 (Du Viver et al. 2015), affected *B. constans* calcification. As a matter of fact, in the studied sections, *B. constans* coccolith size fluctuations mimic CO_2 reconstructions (Fig. 4): a decreasing size trend is observed in the interval with higher CO_2 concentration and, conversely, bigger coccoliths occur around $\delta^{13}C$ peak A, where a ~25% reduction in CO_2 was estimated (Barclay et al. 2010; Jarvis et al. 2011). The subsequent reduction of *B. constans* coccolith dimensions and dwarfism correlates with a further rise in pCO_2 continuing through and after the late phase of OAE 2 (Jarvis et al. 2011). As previously inferred for Mesozoic times (Erba 2006), in the CTBI there was arguably a causal link between levels of CO_2, marine carbonate chemistry and calcite secretion by nannoplankton: when pCO_2 in the ocean-atmosphere system was minimum, production of larger coccoliths was favored by high $CaCO_3$ saturation state. Vice versa, under high CO_2 concentration, a drop in carbonate saturation state induced production of smaller (and less calcified) coccoliths.

In living coccolithophorids, calcification is ruled by an optimum curve; low inorganic carbon content reduces photosynthesis that indirectly limits calcification due to a deficiency of organic molecules needed to construct coccoliths (Krug et al. 2010). Increased inorganic carbon substrate stimulates photosynthesis and calcification reaching maximum values; excess CO_2 release determines low pH that decreases calcification rates (Krug et al. 2010; Bach et al. 2015). The threshold values, below or above, which calcification becomes metabolically unfavorable differ among species due to a species-specific sensitivity to pH conditions (Krug et al. 2010; Bach et al. 2015).

We are conscious that CO_2 injections during OAE 2 occurred during a time interval much longer than modern anthropogenic releases, thus the reduction in carbonate saturation should have been buffered by shallowing of the calcite compensation depth (CCD) with only a minor effect on surface water chemistry. However, the construction of the Caribbean Plateau was sustained for 1-2 million years with several pulses of CO_2 releases and not as a single volcanic eruption. Possibly, as for OAE 1a (Méhay et al. 2009; Erba et al. 2010, 2015) the sum of subsequent large and geologically brief CO_2 emission was responsible for major alteration of the ocean-atmosphere system.

Submarine volcanism of the Caribbean Plateau LIP introduced high concentrations of biolimiting metals during OAE 2 (Snow et al. 2005) that possibly resulted in ocean fertilization and/or poisoning by toxic metals (Leckie et al. 2002; Erba 2004) perhaps influencing coccolith calcification as observed on single modern coccolithophorid species intolerant to cadmium and copper (Brand 1994). We speculate that *B. constans* was sensitive to metal toxicity as previously hypothesized by Erba (2004). Our morphometric results show that this taxon was most receptive, while *Z. erectus*, *D. rotatorius* and *W. barnesiae* were more tolerant. The metal peaks detected at Pueblo (Snow et al. 2005), and Novara di Sicilia (Duncan et al. 2013) are coeval with reduction and dwarfism of *B. constans* coccoliths, remaining small after the metal enrichment around $\delta^{13}C$ peak B through the earliest Turonian. Thus, high metal abundances were possibly a concurring even if not necessarily the prime factor controlling *B. constans* calcification.

Summarizing, in the CTBI, nutrient availability in surface waters *per se* does not seem to be crucial for coccolith calcification because *B. constans* evidence coeval size reductions in the analyzed sections where different trophic levels were reconstructed. Fluctuations in paleotemperatures might be partly responsible for *B. constans* coccolith sizes across OAE 2, with reduced coccolith size under warmer conditions and vice versa, although this correlation does not hold in the aftermath of OAE 2. Morphometric data suggest that ocean chemistry related to the amount of carbon dioxide and/

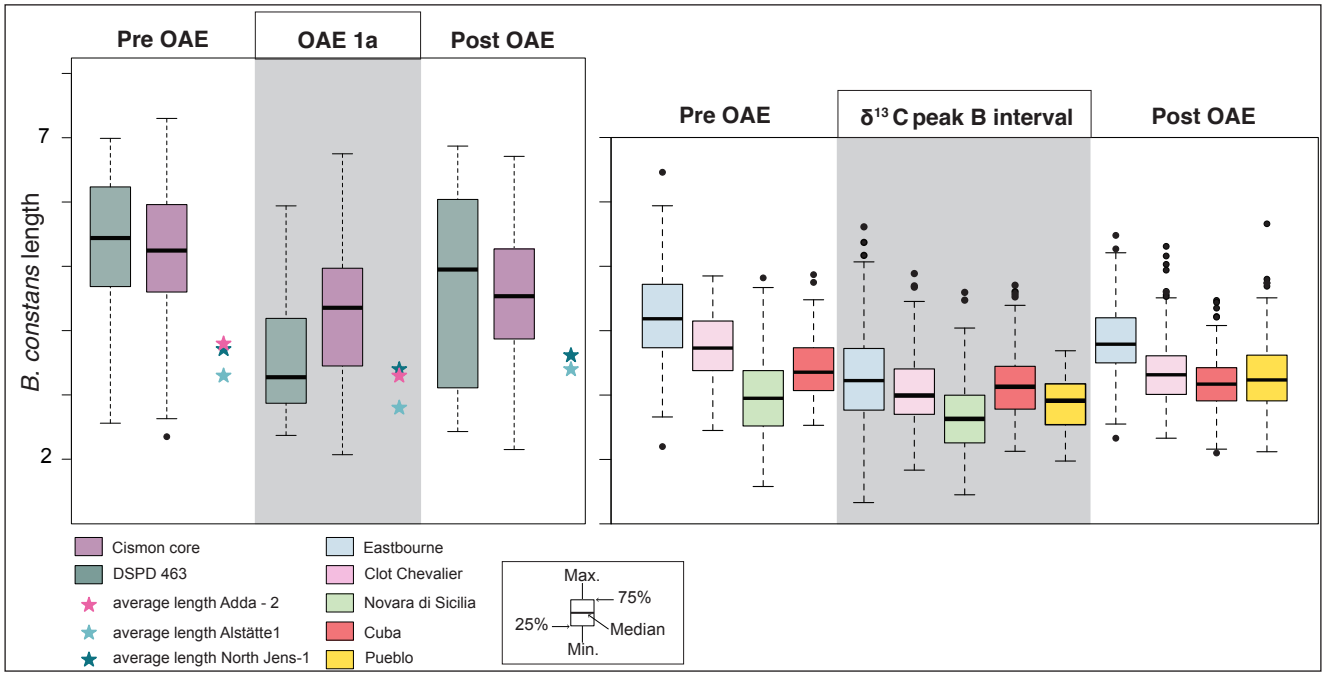

Fig. 5 - Box plots of *B. constans* length across OAE 1a and OAE 2. Data for OAE 1a are from the Cismon core and DSDP Site 463 (Erba et al. 2010). The average length of *B. constans* across OAE 1a are from Adda-2, Alstätte1 and North Jens-1 cores (Lübke & Mutterlose 2016); data for OAE 2 are from Eastbourne, Clot Chevalier, Novara di Sicilia, Pueblo and Cuba sections. Intervals pre-OAE, OAE 1a, $\delta^{13}C$ peak B, post-OAE, are based on $\delta^{13}C$ stratigraphy.

or large quantities of toxic metals played a central role at species-specific level and particularly in *B. constans* coccolith size. However, excess CO_2 in the ocean-atmosphere system was seemingly linked to volcanically-induced warming as well as metal fertilization via hydrothermal plumes during (pulses) of submarine plateau construction.

Comparison among Cretaceous OAEs records

Previous studies performed across other OAEs highlighted size variations of selected nannofossil species. During the Cretaceous, *W. barnesiae* was a cosmopolitan species, common in tropical and subtropical regions and dominant especially in oceanic gyres. It is described as a r-selected opportunistic species (Hardas & Mutterlose 2007) or used as a low productivity indicator (Roth & Krumbach 1986; Erba et al. 1992; Erba 1992, 2004). The data from the early Aptian OAE 1a (Erba et al. 2010; Lübke & Mutterlose 2016), latest Albian OAE 1d (Bornemann & Mutterlose 2006) and OAE 2 (Linnert & Mutterlose 2012; this study) are showing that *W. barnesiae* remains statistically steady in size. However, during OAE 1a, several coccoliths of *W. barnesiae* were affected by some malformation evidenced by strong ellipticity and asymmetry in the interval of most extreme paleoenvironmental stress (Erba et al. 2010). Instead, in all studied sections, no signs of stronger ellipticity or asymmetry were found for the OAE 2 interval. The very little variability measured in *W. barnesiae* specimens in both OAE 1a (Erba et al. 2010; Lübke & Mutterlose 2016) and OAE 2 (Linnert & Mutterlose 2012; this study) possibly suggests that this taxon was most adaptable and only marginally affected by the paleoenvironmental perturbations characterizing Cretaceous OAEs.

During both OAE 1a and OAE 2, *B. constans* appears to be the most sensitive species to the environmental perturbation. The morphometric analyses conducted on *B. constans* and *Z. erectus* across OAE 1a in the Tethys and Pacific Oceans (Erba et al. 2010) as well as in the North Sea and Lower Saxony Basin (Lübke & Mutterlose 2016) highlighted size reduction of their coccoliths during the early stage of OAE 1a in the core of the negative carbon isotope excursion. Contrarily to OAE 2, *B. constans* sizes are smaller in average at higher latitudes (Lübke et al. 2015; Lübke & Mutterlose 2016) compared to lower latitudes (Erba et al. 2010). However, the drastic size decrease of *B. constans* is coeval at high

and low latitudes and occurred in the core of the negative carbon-isotope interval (carbon isotope segment C3) (Erba et al. 2010; Lübke & Mutterlose 2016) reaching comparable minimum *B. constans* coccolith size. The amplitude of size reductions during the earliest phase of OAE 1a is significantly different at lower and higher latitudes, of the order of ~30% versus ~17%, respectively, relative to the interval preceding OAE 1a.

In Fig. 5 the size measurements of *B. constans* across OAE 1a (Erba et al. 2010; Lübke & Mutterlose 2016) and OAE 2 (this study) are compared. *B. constans* display very similar variations in both events, with a drastic decrease during OAEs. A size decrease of *B. constans* coccoliths by 15 % on average, occurred during OAE 2.

The size reduction of *B. constans* coccoliths during OAE 1d was ascribed to cooler surface-waters as indicated by nannofossil-based temperature (Bornemann & Mutterlose 2006). Such temperature influence, however, contradict the conclusions of Linnert & Mutterlose (2012) who observed smaller *Biscutum* coccoliths in the lower Turonian interval characterized by very warm surface temperature. Additionally, during OAE 1a dwarfism occurred in the core of the negative carbon-isotope interval where the highest temperature is reconstructed. Therefore, we do not see a correspondence between lower temperature and smaller size, but possibly the opposite correlation (Fig. 4).

The potential influence of nutrient availability on coccolith size, discussed for OAE 1a (Erba et al. 2010, 2011; Lübke et al. 2015) and OAE 1d (Bornemann & Mutterlose 2006) was documented by general smaller sizes under enhanced fertility. This interpretation is in contrast with the reconstruction by Linnert & Mutterlose (2012) who found larger *Biscutum* coccoliths associated with higher nutrient concentrations in the CTBI. Nutrient availability of surface waters was considered by Corbett & Watkins (2013) to explain changes in nannofossil assemblages across OAE 2 in the WIS. Indeed, the Cuba and Pueblo sections were analyzed and paleoceanographic reconstructions suggest opposite conditions dominated by oligotrophy and eutrophy for the Pueblo and Cuba sections, respectively, during OAE 2. Our data (Fig. 3d, e) document very similar sizes for *B. constans* coccoliths at these two locations and, thus, we infer that fertility was not the primary cause of coccolith size control. Although OAE 1a was also a time of ocean eutrophication (Erba 1994, 2004; Bottini et al. 2015), the time interval of dwarfism corresponds to the climax in the volcanic activity of the Ontong Java Plateau as indicated by Os-isotope (Tejada et al. 2009; Bottini et al. 2012), maximum in CO_2 (Méhay et al. 2009), trace metal concentrations (Erba et al. 2015) and maximum warming (Ando et al. 2008; Bottini et al. 2015) but not to the highest fertility (Bottini et al. 2015).

High run-off due to intensified continental weathering was supposed to have introduced more clastic particles and fresh waters into the sea: muddy and restricted photic zone reduced the availability of light favoring the dominance of small specimens at a regional scale (Lübke & Mutterlose 2016). However, the coeval reduction in sizes at both higher and lower latitudes and at highly diverse oceanic settings during OAE 1a - and specifically in the carbon isotope segment C3 - contradict such interpretation and unambiguously evidences a global paleoenvironmental drive for synchronous coccolith dwarfism of *B. constans*.

The data collected by Erba et al. (2010) and Lübke & Mutterlose (2016) indicate that minimum coccolith size corresponds to most extreme perturbations as recorded by $\delta^{13}C$ negative spike in the early part of OAE 1a. Excess CO_2 concentrations related to the volcanic activity of the Ontong Java Plateau remains the most plausible explanation for coccolith dwarfism in *B. constans, Z. erectus* and *D. rotatorius*, and some malformation in *W. barnesiae* (Erba et al. 2010). Such modifications in size and morphology were interpreted as the species-specific transient response to survive progressively increasing surface-water acidification. It is clear that a combination of paleoclimatic and paleoceanographic triggers concurred in stressing the oceanic ecosystem, but, as discussed by Erba et al. (2011), ocean acidification under excess volcanic CO_2 seems to be the requisite or determinant of species-specific size reduction and malformation during OAE 1a, because coccolith dwarfism has not been documented during other Cretaceous cases of high fertility independent from OAEs.

During OAE 2, reconstruction of pCO_2 from the stomatal index suggests an increase of about 600 ppm reaching values of about 900-1000 ppm (Barclay et al. 2010). Pogge von Strandmann et al. (2013) calculated the amount of CO_2 sequestered from the continental weathering (~ 4-8 x 10^4 Gt

CO_2) in agreement with previous calculation of the amount of CO_2 emitted in the first phase of construction of the Caribbean Plateau (7-12 x 10^4 Gt CO_2) (Kuroda et al. 2007). It is therefore conceivable that size reduction of *B. constans* coccoliths (Fig. 4), reflects a progressive acidification of surface-waters induced by large emissions of volcanic CO_2. Proxy data (e.g. Erba & Tremolada 2004; Méhay et al. 2009) suggest that during OAE 1a CO_2 was emitted in subsequent individual volcanic pulses reaching a concentration of about 1000-2000 ppm. In both OAEs, thus, the occurrence of *B. constans* dwarf coccoliths correlates with excess CO_2 suggesting that concentrations above threshold values possibly become adverse for calcification of sensitive Cretaceous coccolithophore species, in analogy to results of laboratory experiments (Riebesell et al. 2000; Krug et al. 2011; Bach et al. 2012; Bach et al. 2015). Calcification must be a beneficial process for coccolithophore algae because this high energy-consuming process remained stable in coccolithophore evolution from its appearance in the Triassic (Young & Henriksen 2003). However, during the most extreme intervals such as OAEs, a decrease of the pH might have favored other groups other than coccolithophore algae (Bach et al. 2015). During OAE 2, in fact, in the interval characterized by the major perturbation ($\delta^{13}C$ peak B) the decrease in *B. constans* is paralleled by a strong increase in calcisphere percentages (Pearce et al. 2009). This can be interpreted as an inability of *B. constans* to properly calcify and adapt to a new carbonate chemistry conditions, facilitating the spread of other more competitive functional groups such as dinoflagellates.

One potential factor that may have affected coccolith calcification in addition to CO_2-induced ocean acidification is the concentration of toxic metals. Indeed, we notice that during both OAE 1a (Larson & Erba 1999; Erba et al. 2015) and OAE 2 (Snow et al. 2005; Duncan et al. 2013) there were large injections of trace metals associated with hydrothermal plumes during the construction of submarine LIPs (Neal et al. 2008). Abnormal quantities of biolimiting but also toxic metals might have had positive and negative feedbacks in coccolith production and, particularly, on size of *B. constans* coccoliths. Metal toxicity is known for living nannoplankton: cadmium can inhibit calcification and copper is not tolerated by some coccolithophore species (Brand 1994). As speculated by Erba (2004) perhaps, poisoning by toxic metals affected calcareous nannoplankton in the Cretaceous, inducing some extinctions, abundance drop and species-specific coccolith dwarfism.

Conclusions

Morphometric analyses of selected nannofossil taxa across OAE 2 in various geological settings revealed differential species-specific patterns. Coccolith size variations of *D. rotatorius*, *W. barnesiae* and *Z. erectus* result to be minimal and substantially unrelated to OAE 2 paleoenvironmental stresses. Conversely, *B. constans* coccolith morphometric analyses identified size variations coeval with specific phases of environmental pressure. Size fluctuations across OAE 2 are similar and synchronous in all the analyzed sections located at great distance, in different oceans and settings.

The quantitative characterization of coccolith size and morphology in the intervals preceding, coeval and postdating OAE 2 assessed the occurrence of a relationship between calcification of *B. constans* and paleoenvironmental perturbations. In fact, during OAE 2, *B. constans* coccoliths show a general decrease in mean size followed by a partial recovery at the end of the event, but dimensions remained smaller than in the interval preceding the main perturbation. At higher resolution, coeval decreases and increases in coccolith size correspond to individual paleoenvironmental changes across OAE 2. We underline that *B. constans* dwarfism is observed in complete specimens with no corrosion in their outline and, therefore, cannot be explained as an artifact of diagenesis.

The comparison with morphometric data available for the early Aptian and latest Albian OAEs confirms that *B. constans* was most affected by stressing conditions and repeatedly underwent size reduction with evidence of temporary dwarfism. This suggests that presumably the same paleoenvironmental factors (or the same combination of ecosystem changes) controlled calcification of *B. constans* coccoliths during OAE 1a, OAE 1d and OAE 2. However, the amplitude of *B. constans* coccolith reduction is different for OAE 1a and OAE 2, being larger for the former event.

Z. erectus and *D. rotatorius* display a less-expressed decrease in size during OAE 1a and insig-

nificant or scattered changes across OAE 2; dwarfism of these taxa was detected only in the interval of climax perturbation during the early Aptian Selli Event. The very little variability measured in *W. barnesiae* size indicate that this taxon was most adaptable and only marginally affected by the paleoenvironmental stress characterizing Cretaceous OAEs: while pronounced ellipticity was taken as evidence of malformation of *W. barnesiae* coccoliths during OAE 1a, negligible variations in ellipticity were observed across OAE 2, perhaps because of an attenuated degrees of perturbation.

Our results reinforce and implement paleoecological reconstructions of abiotic and biotic parameters somehow influencing coccolith secretion across OAE 2, OAE 1d and OAE 1a allowing the evaluation of the factor, or combination of factors, inducing *B. constans* coccolith dwarfism in subsequent episodes of paleoenvironmental perturbation. Temperature and nutrient availability in surface waters do not seem to have been decisive for *B. constans* coccolith size, but ocean chemistry related to the amount of CO_2 concentrations and carbonate saturation state, played a central role in coccolith production by *B. constans* with a repetitive reduction in size. Species-specific coccolith dwarfism seems to be the response of nannoplankton to ocean acidification during both OAE 1a and OAE 2 to survive lower pH.

Massive emissions of volcanic CO_2 during the Caribbean Plateau construction across OAE 2 (Neal et al. 2008) arguably induced ocean acidification that was detrimental to some calcareous nannoplankton species, with temporary production of dwarf *B. constans* coccoliths. Hydrothermal plumes introduced biolimiting metals that fertilized the global ocean, but also pumped in toxic metals that might have disturbed the functioning of some intolerant species, thus affecting their biocalcification.

Comparison of our results with data available for OAE 1a and OAE 1d indicate that analogous causes have induced similar response at different times in the Cretaceous. The OAEs indicate that past oceanic perturbations were severe and that the species-specific production of dwarf coccoliths possibly represents adjustment of some individual taxa to survive hostile ecosystems. This study further suggests that *B. constans* was the mid-Cretaceous taxon most sensitive to ocean chemistry, while other species (*Z. erectus*, *D. rotatorius* and *W. barnesiae*) were affected only at highest degrees of perturbation. It seems that calcareous nannoplankton have been resilient to pH changes, excess toxic metals, global warming and nutrification episodes, but it is certainly possible that the rate of change was decisive for coccolithophore adaptation. The geological record indicates that, at wide spatial scale, calcareous nannoplankton could adjust to high pCO_2, but past changes occurred over tens of thousands of years, giving enough time to adapt.

Acknowledgements. We thank Tim Bralower and Bob Duncan for sharing samples from the WIS sections, and Hugh Jenkyns for providing samples from the Clot Chevalier section. We thank the Editor, Isabella Raffi, and two anonymous reviewers for their valuable comments and suggestions on the manuscript. The research was funded through MIUR-PRIN 2011 (Ministero dell'Istruzione, dell'Università e della Ricerca–Progetti di Ricerca di Interesse Nazionale) to E. Erba, and through SIR-2014 (Ministero dell'Istruzione, dell'Università e della Ricerca–Scientific Independence of young Researchers) to C. Bottini. G. Faucher was supported by Fondazione Fratelli Confalonieri.

References

Ando A., Kaiho K., Kawahata H. & Kakegawa T. (2008) - Timing and magnitude of early Aptian extreme warming: unraveling primary $\delta^{18}O$ variation in indurated pelagic carbonates at Deep Sea Drilling Project Site 463, central Pacific Ocean. *Palaeogeogr., Palaeoclimatol., Palaeoecol.,* 260(3): 463-476, doi:10.1016/j.palaeo.2007.12.007.

Bach L.T., Bauke C., Meier K. J.S., Riebesell U. & Schulz K.G. (2012) - Influence of changing carbonate chemistry on morphology and weight of coccoliths formed by *Emiliania huxleyi*. *Biogeosciences (BG),* 9(8): 3449-3463, doi:10.1016/j.pocean.2015.04.012.

Bach L.T., Riebesell U., Gutowska M.A., Federwisch L. & Schulz K.G. (2015) - A unifying concept of coccolithophore sensitivity to changing carbonate chemistry embedded in an ecological framework. *Progr. Oceanogr.,* 135: 125-138, doi:10.1016/j.pocean.2015.04.012.

Barclay R.S., McElwain J.C. & Sageman B.B (2010) - Carbon sequestration activated by a volcanic CO_2 pulse during Ocean Anoxic Event 2. *Nat. Geosci.*, 3(3): 205-208, doi:10.1038/ngeo757.

Beaufort L., Probert I., de Garidel-Thoron T., Bendif E.M., Ruiz-Pino D., Metzl N., Goyet C., Buchet N., Coupel P., Grelaud M., Rost B., Rickaby R.E.M. & De Vargas C. (2011) - Sensitivity of coccolithophores to carbonate chemistry and ocean acidification. *Nature*, 476(7358): 80-83, doi:10.1038/nature10295.

Blättler C.L., Jenkyns H.C., Reynard L.M. & Henderson G.M. (2011) - Significant increases in global weathering during Oceanic Anoxic Events 1a and 2 indicated by calcium isotopes. *Earth Planet. Sci. Lett.*, 309(1): 77-88, doi:10.1016/j.epsl.2011.06.029.

Bornemann A. & Mutterlose J. (2006) - Size analyses of the coccolith species *Biscutum constans* and *Watznaueria barnesiae* from the Late Albian "Niveau Breistroffer"(SE France): taxonomic and palaeoecological implications. *Geobios*, 39(5): 599-615, doi:10.1016/j.geobios.2005.05.005.

Bottini C., Cohen A.S., Erba E., Jenkyns H.C. & Coe A.L. (2012) - Osmium-isotope evidence for volcanism, weathering, and ocean mixing during the early Aptian OAE 1a. *Geology*, 40(7): 583-586, doi: 10.1130/G33140.

Bottini C., Erba E., Tiraboschi D., Jenkyns, H.C., Schouten S. & Sinninghe Damsté J.S. (2015) - Climate variability and ocean fertility during the Aptian Stage. *Clim. Past,* 11(3), doi:10.5194/cp-11-383-2015.

Bowman A.R. & Bralower T.J. (2005). Paleoceanographic significance of high-resolution carbon isotope records across the Cenomanian-Turonian boundary in the Western Interior and New Jersey coastal plain, USA. *Mar. Geol.*, 217, 3: 305-321, doi:10.1016/j.margeo.2005.02.010.

Bown P.R. & Young J.R. (1998) - Introduction. In: Bown P.R. (Ed.) - Calcareous nannofossil biostratigraphy: 1-15. British Micropalentol. Soc. Publ. Series, Kluver Academic Publ., University press Cambridge, UK.

Bralower T.J. (1988) - Calcareous nannofossil biostratigraphy and assemblages of the Cenomanian-Turonian boundary interval: Implications for the origin and timing of oceanic anoxia. *Paleoceanography*, 3(3): 275-316.

Brand L.E. (1994) - Physiological ecology of marine coccolithophores. In: Winter A. & Siesser W.G. (Eds) - Coccolithophores: 39-49. Cambridge Univ. Press, Cambridge.

Burnett J.A., Gallagher L.T. & Hampton M.J. (1998) - Upper cretaceous. Calcareous nannofossil biostratigraphy: 132-199.

Corbett M.J. & Watkins D.K. (2013) - Calcareous nannofossil paleoecology of the mid-Cretaceous Western Interior Seaway and evidence of oligotrophic surface waters during OAE2. *Palaeogeogr., Palaeoclimatol., Palaeoecol.*, 392: 510-523, doi:10.1016/j.palaeo.2013.10.007.

Corbett M.J., Watkins D.K. & Pospichal J.J. (2014) - A quantitative analysis of calcareous nannofossil bioevents of the Late Cretaceous (Late Cenomanian-Coniacian) Western Interior Seaway and their reliability in established zonation schemes. *Mar. Micropaleontol.*, 109: 30-45, doi:10.1016/j.marmicro.2014.04.002.

Desmares D., Grosheny D., Beaudoin B., Gardin S. & Gauthier-Lafaye F. (2007) - High resolution stratigraphic record constrained by volcanic ash beds at the Cenomanian-Turonian boundary in the Western Interior Basin, USA. *Cret. Res.*, 28(4): 561-582, doi:10.1016/j.cretres.2006.08.009.

Duncan R., Snow L. & Scopelliti G. (2013) - The Caribbean Plateau and OAE 2: Resolution of Timing and Trace Metal Release. *Mineral. Mag.,* 77(5): 1018, paper presented at 23rd Goldschmidt Conference, 2013, Florence.

Du Vivier A.D., Selby D., Sageman B.B., Jarvis I., Gröcke D. R. & Voigt S. (2014) - Marine $^{187}Os/^{188}Os$ isotope stratigraphy reveals the interaction of volcanism and ocean circulation during Oceanic Anoxic Event 2. *Earth Planet. Sci. Lett.*, 389: 23-33, doi:10.1016/j.epsl.2013.12.024.

Du Vivier A.D., Jacobson A.D., Lehn G.O., Selby D., Hurtgen M.T. & Sageman B.B. (2015) - Ca isotope stratigraphy across the Cenomanian-Turonian OAE 2: Links between volcanism, seawater geochemistry, and the carbonate fractionation factor. *Earth Planet. Sci. Lett.*, 416: 121-131, doi:10.1016/j.epsl.2015.02.001.

Eleson J.W. & Bralower T.J. (2005) - Evidence of changes in surface water temperature and productivity at the Cenomanian/Turonian Boundary. *Micropaleontology*, 51(4): 319-332, doi: 10.2113/gsmicropal.51.4.319.

Erba E. (1992) - Middle Cretaceous calcareous nannofossils from the Western Pacific (ODP Leg 129): evidence for paleoequatorial crossings. In: Larson, R.L & Lancelot Y. (Eds) - *Proc. ODP Sci. Results*, 129: 189-201.

Erba E. (1994) - Nannofossils and superplumes: the early Aptian "nannoconid crisis". *Paleoceanography*, 9(3): 483-501, doi: 10.1029/94PA00258.

Erba E. (2004) - Calcareous nannofossils and Mesozoic oceanic anoxic events. Marine *Micropaleontology*, 52(1): 85-106, doi:10.1016/j.marmicro.2004.04.007.

Erba E. (2006) - The first 150 million years history of calcareous nannoplankton: biosphere-geosphere interactions. *Palaeogeogr., Palaeoclimatol., Palaeoecol.*, 232(2): 237-250, doi:10.1016/j.palaeo.2005.09.013.

Erba E. & Tremolada F. (2004) - Nannofossil carbonate fluxes during the Early Cretaceous: Phytoplankton response to nutrification episodes, atmospheric CO_2 and anoxia. *Paleoceanography*, 19(1), doi: 10.1029/2003PA000884.

Erba E., Castradori D., Guasti G. & Ripepe M. (1992) - Calcareous nannofossils and Milankovitch cycles: the example of the Albian Gault Clay Formation (southern England). *Palaeogeogr., Palaeoclimatol., Palaeoecol.*, 93(1): 47-69, doi:10.1016/0031-0182(92)90183-6f.

Erba E., Bottini C., Weissert H. J. & Keller C. E. (2010) - Calcareous nannoplankton response to surface-water acidification around Oceanic Anoxic Event 1a. *Science*, 329(5990): 428-432, doi: 10.1126/science.1188886.

Erba E., Bottini C., Weissert H.J. & Keller C.E. (2011) - Response to comment on "Calcareous nannoplankton response to surface-water acidification around Oceanic Anoxic Event 1a". *Science*, 332(6026): 175-175, doi: 10.1126/science.1199608.

Erba E., Duncan R.A., Bottini C., Tiraboschi D., Weissert H., Jenkyns H.C. & Malinverno A. (2015) - Environmental Consequences of Ontong Java Plateau and Kerguelen Plateau Volcanism. *GSA Spec. Pap.,* 511, doi:10.1130/2015.2511.

Falzoni F., Petrizzo M.R., Jenkyns H.C., Gale A.S. & Tsikos H. (2016) - Planktonic foraminiferal biostratigraphy and assemblage composition across the Cenomanian-Turonian boundary interval at Clot Chevalier (Vocontian Basin, SE France). *Cret. Res.*, 59: 69-97, doi:10.1016/j.cretres.2015.10.028.

Föllmi K.B. (2012) - Early Cretaceous life, climate and anoxia. *Cret. Res.,* 35: 230-257, doi:10.1016/j.cretres.2011.12.005.

Forster A., Schouten S., Moriya K., Wilson P.A. & Sinninghe Damsté J.S. (2007) - Tropical warming and intermit-

tent cooling during the Cenomanian/Turonian oceanic anoxic event 2: Sea surface temperature records from the equatorial Atlantic. *Paleoceanography*, 22(1), doi: 10.1029/2006PA001349.

Gale A.S. (1995) - Cyclostratigraphy and correlation of the Cenomanian stage in Western Europe. *Geol. Soc., London, Spec. Pub.*, 85(1): 177-197, doi: 10.1144/GSL.SP.1995.085.01.11.

Gale A.S. (1996) - Turonian correlation and sequence stratigraphy of the Chalk in southern England. *Geol. Soc., London, Spec. Pub.*, 103(1): 177-195, doi: 10.1144/GSL.SP.1996.103.01.10.

Gale A.S., Hancock J.M. & Kennedy W.J. (1999) - Biostratigraphical and sequence correlation of the Cenomanian successions in Mangyshlak (W. Kazakhstan) and Crimea (Ukraine) with those in southern England. *Bull.-Inst. roy. sci. nat. Belgique. Sci. Terre*, 69: 67-86.

Gambacorta G., Jenkyns H.C., Russo F., Tsikos H., Wilson P. A., Faucher G. & Erba E. (2015) - Carbon-and oxygen-isotope records of mid-Cretaceous Tethyan pelagic sequences from the Umbria-Marche and Belluno Basins (Italy). *Newsl. Strat.*, 48(3): 299-323, doi:http://dx.doi.org/10.1127/nos/2015/0066.

Hay W.W. (2009) - Cretaceous oceans and ocean modeling. In: Hu X., Wang C., Scott R.W., Wagreich M. & Jansa L. (Eds) - Cretaceous Oceanic Red Beds: Stratigraphy, Composition, Origins and Paleoceanographic and Paleoclimatic Significance 91: 243-271. SEPM (Society for Sedimentary Geology) Special Publication.

Hardas P. & Mutterlose J. (2007) - Calcareous nannofossil assemblages of Oceanic Anoxic Event 2 in the equatorial Atlantic: Evidence of an eutrophication event. *Mar. Micropaleontol.*, 66(1): 52-69, doi:10.1016/j.marmicro.2007.07.007.

Hattin D.E. (1975) - Petrology and origin of fecal pellets in Upper Cretaceous strata of Kansas and Saskatchewan. *J. Sedim. Res.*, 45(3): 686-696.

Hattin D.E. (1985) - Distribution and significance of widespread, time-parallel pelagic limestone beds in Greenhorn Limestone (Upper Cretaceous) of the central Great Plains and southern Rocky Mountains. Limestone (Upper Cretaceous) of the Central Great Plains and Southern Rocky Mountains. In: Pratt L.M., Kauffman E.G. & Zelt F.B. (Eds) - Fine-Grained Deposits and Biofacies of the Cretaceous Western Interior Seaway: evidence of Cyclic Sedimentary Processes, 4: 28-37, SEPM Field Trip Guidebook.

Hoffmann L.J., Breitbarth E., Ardelan M.V., Duggen S., Olgun N., Hassellöv M. & Wängberg S.Å. (2012) - Influence of trace metal release from volcanic ash on growth of *Thalassiosira pseudonana* and *Emiliania huxleyi*. *Mar. Chem.*, 132: 28-33, doi:10.1016/j.marchem.2012.02.003.

Herrmann S. & Thierstein H.R. (2012) - Cenozoic coccolith size changes-evolutionary and/or ecological controls*? Palaeogeogr., Palaeoclimatol., Palaeoecol.*, 333*:* 92-106.

Herrmann S., Weller A.F., Henderiks J. & Thierstein H.R. (2012) - Global coccolith size variability in Holocene deep-sea sediments. *Mar. Micropaleontol.*, 82: 1-12.

Jarvis I.A.N., Gale A.S., Jenkyns H.C. & Pearce M.A. (2006) - Secular variation in Late Cretaceous carbon isotopes: a new $\delta^{13}C$ carbonate reference curve for the Cenomanian-Campanian (99.6-70.6 Ma). *Geol. Mag.*, 143(05): 561-608, doi: http://dx.doi.org/10.1017/S0016756806002421.

Jarvis I., Lignum J.S., Gröcke D.R., Jenkyns H.C. & Pearce M.A. (2011) - Black shale deposition, atmospheric CO_2 drawdown, and cooling during the Cenomanian-Turonian Oceanic Anoxic Event. *Paleoceanography*, 26(3), doi: 10.1029/2010PA002081.

Jenkyns H.C. (2010) - Geochemistry of oceanic anoxic events. *Geochem., Geophys., Geosyst.*, 11, Q03004, doi:10.1029/2009GC002788.

Jenkyns H.C., Dickson A.J., Ruhl M. & Van Den Boorn S. H. (2016) - Basalt-seawater interaction, the Plenus Cold Event, enhanced weathering and geochemical change: Deconstructing OAE 2 (Cenomanian-Turonian, Late Cretaceous). *Sedimentology*, doi: 10.1111/sed.12305.

Keller G. & Pardo A. (2004) - Age and paleoenvironment of the Cenomanian-Turonian global stratotype section and point at Pueblo, Colorado. *Mar. Micropaleontol.*, 51(1): 95-128, doi:10.1016/j.marmicro.2003.08.004.

Kennedy W., Walaszczyk I. & Cobban W. (2000) - Pueblo, Colorado, USA, candidate Global Boundary Stratotype Section and Point for the base of the Turonian Stage of the Cretaceous and for the base of the middle Turonian Substage, with a revision of the Inoceramidae (Bivalvia). *Acta Geol. Pol.*, 50: 295-334.

Kennedy W.J., Walaszczyk I. & Cobban W.A. (2005) - The global boundary stratotype section and point for the base of the Turonian stage of the Cretaceous: Pueblo, Colorado, USA. *Episodes*, 28(2): 93-104.

Kuroda J., Ogawa N.O., Tanimizu M., Coffin M.F., Tokuyama H., Kitazato H. & Ohkouchi N. (2007) - Contemporaneous massive subaerial volcanism and late cretaceous Oceanic Anoxic Event 2. *Earth Plan. Sci. Lett.*, 256(1): 211-223, doi:10.1016/j.epsl.2007.01.027.

Krug S., Schulz K. & Riebesell U. (2011) - Effects of changes in carbonate chemistry speciation on *Coccolithus braarudii*: a discussion of coccolithophorid sensitivities. *Biogeosciences* (BG), 8: 771-777, doi:10.5194/bg-8-771-2011.

Larson R.L. & Erba E. (1999) - Onset of the Mid-Cretaceous greenhouse in the Barremian-Aptian: igneous events and the biological, sedimentary, and geochemical responses. *Paleoceanography*, 14(6): 663-678, doi: 10.1029/1999PA900040.

Leckie R.M. (1985) - Foraminifera of the Cenomanian-Turonian Boundary Interval, Greenhorn Formation, Rock Canyon Anticline, Pueblo, Colorado in: Society of Economic Paleontologists and Mineralogists Field Trip Guidebook 4: 139-155. Midyear Meeting, Golden, Colorado.

Leckie R.M., Bralower T.J. & Cashman R. (2002) - Oceanic anoxic events and plankton evolution: Biotic response to tectonic forcing during the mid-Cretaceous. *Paleoceanography*, 17(3): 13-1, doi: 10.1029/2001PA000623.

Lees J.A., Bown P.R. & Mattioli E. (2005) - Problems with proxies? Cautionary tales of calcareous nannofossil paleoenvironmental indicators. *Micropaleontology*, 51(4): 333-343.

Linnert C. & Mutterlose J. (2012) - Biometry of Cenomanian-Turonian placoliths: a proxy for changes of fertility and surface-water temperature? *Lethaia*, 46(1): 82-97, doi: 10.1111/j.1502-3931.2012.00323.x.

Linnert C. & Mutterlose J. (2015) - Boreal early Turonian calcareous nannofossils from nearshore settings-implications for Paleoecology. *Palaios*, 30(10): 728-742 doi: 10.2110/palo.2014.099.

Linnert C., Mutterlose J. & Erbacher J. (2010) - Calcareous nannofossils of the Cenomanian/Turonian boundary interval from the Boreal Realm (Wunstorf, northwest Germany). *Mar. Micropaleontol.*, 74(1): 38-58, doi:10.1016/j.marmicro.2009.12.002.

Linnert C., Mutterlose J. & Mortimore R. (2011) - Calcareous nannofossils from Eastbourne (southeastern England) and the paleoceanography of the Cenomanian-Turonian Boundary interval. *Palaios*, 26(5): 298-313, doi: 10.2110/palo.2010.p10-130r.

Lübke N. & Mutterlose J. (2016) - The impact of OAE 1a on marine biota deciphered by size variations of coccoliths. *Cret. Res.*, 61: 169-179.

Lübke N., Mutterlose J. & Bottini C. (2015) - Size variations of coccoliths in Cretaceous oceans - A result of preservation, genetics and ecology? *Mar. Micropaleontol.*, 117: 25-39, doi:10.1016/j.marmicro.2015.03.002.

Méhay S., Keller C.E., Bernasconi S.M., Weissert H., Erba E., Bottini C. & Hochuli P.A. (2009) - A volcanic CO_2 pulse triggered the Cretaceous Oceanic Anoxic Event 1a and a biocalcification crisis. *Geology*, 37(9): 819-822, doi:10.1130/G30100A.1.

Müller M.N., Kısakürek B., Buhl D., Gutperlet R., Kolevica A., Riebesell U., Heather S. & Eisenhauer A. (2011) - Response of the coccolithophores *Emiliania huxleyi* and *Coccolithus braarudii* to changing seawater Mg^{2+} and Ca^{2+} concentrations: Mg/Ca, Sr/Ca ratios and $\delta^{44/40}Ca$, $\delta^{26/24}Mg$ of coccolith calcite. *Geochim. Cosmochim. Acta*, 75(8): 2088-2102, doi:10.1016/j.gca.2011.01.035.

Müller M.N., Beaufort L., Bernard O., Pedrotti M.L., Talec A. & Sciandra A. (2012) - Influence of CO_2 and nitrogen limitation on the coccolith volume of *Emiliania huxleyi* (Haptophyta). *Biogeosciences*, 9(10): 4155-4167, doi:10.5194/bg-9-4155-2012.

Neal C.R., Coffin M.F., Arndt N.T., Duncan R.A., Eldholm O., Erba E., Farnetani C., Fitton J.G., Ingle S.P., Ohkouchi N., Rampino M.R., Reichow M.K., Self S. & Tatsumi Y. (2008) - Investigating large igneous province formation and associated paleoenvironmental events: a white paper for scientific drilling. *Scientific Drilling*, 6: 4-18, doi:10.04/iodp.sd.6.01. 008f

Paul C.R.C., Lamolda M.A., Mitchell S.F., Vaziri M.R., Gorostidi A. & Marshall J.D. (1999) - The Cenomanian-Turonian boundary at Eastbourne (Sussex, UK): a proposed European reference section. *Palaeogeogr., Palaeoclimatol., Palaeoecol.*, 150(1): 83-121, doi:10.1016/S0031-0182(99)00009-7.

Pearce M.A., Jarvis I. & Tocher B.A. (2009) - The Cenomanian-Turonian boundary event, OAE2 and palaeoenvironmental change in epicontinental seas: new insights from the dinocyst and geochemical records. *Palaeogeogr., Palaeoclimatol., Palaeoecol.*, 280(1): 207-234, doi:10.1016/j.palaeo.2009.06.012.

Pogge von Strandmann P.A.P., Jenkyns H.C. & Woodfine R.G. (2013) - Lithium isotope evidence for enhanced weathering during Oceanic Anoxic Event 2. *Nat. Geosc.*, 6(8): 668-672, doi:10.1038/ngeo1875.

Pratt L. M. (1985) - Isotopic studies of organic matter and carbonate in rocks of the Greenhorn marine cycle. In: Fine-Grained deposits and biofacies of the Cretaceous Greenhorn Formation, Pueblo, Colorado. *Am. Assoc. Pet. Bull.,* 68: 1146-1159.

Pratt L.M., Arthur M.A., Dean W.E. & Scholle P.A. (1993) - Paleo-oceanographic cycles and events during the Late Cretaceous in the Western Interior Seaway of North America. In: Evolution of the Western Interior Basin, 39: 333-354. Geol. Ass. Canada, Spec. Pap.

Riebesell U., Zondervan I., Rost B., Tortell P.D., Zeebe R.E. & Morel F.M. (2000) - Reduced calcification of marine plankton in response to increased atmospheric CO_2. *Nature*, 407: 6802, 364-367, doi:10.1038/35030078.

Roth P.H. & Krumbach K.R. (1986) - Middle Cretaceous calcareous nannofossil biogeography and preservation in the Atlantic and Indian Oceans: implications for paleoceanography. *Mar. Micropaleontol.*, 10(1): 235-266.

Russo F. (2014) - Calcareous nannofossil revised biostratigraphy of the latest Albian-earliest Campanian time interval (late Cretaceous). PhD thesis, Università degli Studi di Milano.

Sageman B.B., Meyers S.R. & Arthur M.A. (2006) - Orbital time scale and new C-isotope record for Cenomanian-Turonian boundary stratotype. *Geology*, 34(2): 125-128, doi: 10.1130/G22074.1.

Schlanger S.O. & Jenkyns H.C. (1976) - Cretaceous oceanic anoxic events: causes and consequences. *Geol. Mijnbouw*, 55(3-4): 179-184.

Scopelliti G., Bellanca A. Erba E., Jenkyns H.C., Neri R., Tamagnini P., Luciani V. & Masetti D. (2008) - Cenomanian-Turonian carbonate and organic-carbon isotope records, biostratigraphy and provenance of a key section in NE Sicily, Italy: palaeoceanographic and palaeogeographic implications. *Palaeogeogr., Palaeoclimatol., Palaeoecol.,* 265(1): 59-77, doi:10.1016/j.palaeo.2008.04.022.

Sett S., Bach L.T., Schulz K.G., Koch-Klavsen S., Lebrato M. & Riebesell U. (2014) - Temperature modulates coccolithophorid sensitivity of growth, photosynthesis and calcification to increasing seawater pCO_2. *PLOS ONE* 9, e88308, http://dx.doi.org/10.1371/journal.pone.0088308

Sinninghe Damsté J.S., Kuypers M.M.M., Pancost R.D. & Schouten S. (2008) - The carbon isotopic response of algae, (cyano)bacteria, archaea and higher plants to the late Cenomanian perturbation of the global carbon cycle: Insights from biomarkers in black shales from the Cape Verde Basin (DSDP Site 367), *Org. Geochem.*, 39, 1703-1718, doi:10.1016/j. orggeochem.2008.01.012.

Sissingh W. (1977) - Biostratigraphy of Cretaceous calcareous nannoplankton. *Geol. Mijnbouw,* 56: 37-65.

Snow L.J., Duncan R.A. & Bralower T.J. (2005) - Trace element abundances in the Rock Canyon Anticline, Pueblo, Colorado, marine sedimentary section and their relationship to Caribbean plateau construction and oxygen anoxic event 2. *Paleoceanography*, doi:10.1029/2004PA001093, 20, 3.

Tejada M.L.G., Suzuki K., Kuroda J., Coccioni R., Mahoney J., John. J., Ohkouchi N., Sakamoto T. & Tatsumi Y. (2009) - Ontong Java Plateau eruption as a trigger for the early Aptian oceanic anoxic event. *Geology*, 37(9): 855-858, doi: 10.1130/G25763A.1.

Thierstein H.R. (1980) - Selective dissolution of Late Cretaceous and earliest Tertiary calcareous nannofossils: experimental evidence. *Cret. Res.*, 1(2): 165-176.

Thierstein H.R. & Roth P.H. (1991) - Stable isotopic and carbonate cyclicity in Lower Cretaceous deep-sea sediments: dominance of diagenetic effects. *Mar. Geol.*, 97(1): 1-34.

Tsikos H., Jenkyns H.C., Walsworth-Bell B., Petrizzo M.R., Forster A., Kolonic S., Erba E., Premoli Silva I., Baas M. Wagner T. & Damsté J.S. (2004) - Carbon-isotope stratigraphy recorded by the Cenomanian-Turonian Oceanic Anoxic Event: correlation and implications based on three key localities. *J. Geol. Soc.*, 161(4): 711-719, doi: 10.1144/0016-764903-077.

Voigt S., Gale A. S. & Flögel S. (2004) - Midlatitude shelf seas in the Cenomanian-Turonian greenhouse world: Temperature evolution and North Atlantic circulation. *Paleoceanography*, 19(4), doi: 10.1029/2004PA001015.

Wilpshaar M., Leereveld H. & Visscher H. (1997) - Early Cretaceous sedimentary and tectonic development of the Dauphinois Basin (SE France). *Cret. Res.*, 18(3): 457-468, doi:10.1006/cres.1997.0062.

Young J. R. & Henriksen K. (2003) - Biomineralization within vesicles: the calcite of coccoliths. *Reviews mineral. geochem.,* 54(1): 189-215, doi: 10.2113/0540189.